

7981

Abstract

Plant phenological development is orchestrated through subtle changes in photoperiod, temperature, soil moisture and nutrient availability. Presently, the exact timing of plant development stages and their response to climate and management practices are crudely represented in land surface models. As visual observations of phenology are laborious, there is a need to supplement long-term observations with automated techniques such as those provided by digital repeat photography at high temporal and spatial resolution. We present the first synthesis from a growing observational network of digital cameras installed on towers across Europe above deciduous and evergreen forests, grasslands and croplands, where vegetation and atmosphere CO₂ fluxes are measured continuously. Using colour indices from digital images and using piecewise regression analysis of time-series, we explored whether key changes in canopy phenology could be detected automatically across different land use types in the network. The piecewise regression approach could capture the start and end of the growing season, in addition to identifying striking changes in colour signals caused by flowering and management practices such as mowing. Exploring the dates of green up and senescence of deciduous forests extracted by the piecewise regression approach against dates estimated from visual observations we found that these phenological events could be detected adequately (RMSE < 8 and 11 days for leaf out and leaf fall respectively). We also investigated whether the seasonal patterns of red, green and blue colour fractions derived from digital images could be modelled mechanistically using the PROSAIL model parameterised with information of seasonal changes in canopy leaf area and leaf chlorophyll and carotenoid concentrations. From a model sensitivity analysis we found that variations in colour fractions, and in particular the late spring “green hump” observed repeatedly in deciduous broadleaf canopies across the network, are essentially dominated by changes in the respective pigment concentrations. Using the model we were able to explain why this spring maximum in green signal is often observed out of phase with the maximum period of canopy photosynthesis in

7982

ecosystems across Europe. Coupling such quasi-continuous digital records of canopy colours with co-located CO₂ flux measurements will improve our understanding of how changes in growing season length are likely to shape the capacity of European ecosystems to sequester CO₂ in the future.

5 1 Introduction

Within Europe continuous flux measurements of CO₂, water and energy exchange between ecosystems and the atmosphere started in the early 1990s at a handful of forest sites (Janssens et al., 2001; Valentini et al., 2000). Nowadays, through the realisation of large European programmes such as EUROFLUX and CARBOEUROPE-IP amongst others, the number of natural and managed terrestrial ecosystems where the dynamics of water and CO₂ fluxes are monitored continuously has increased tremendously (Baldocchi, 2014; Baldocchi et al., 2001), and that number is set to be maintained in Europe for at least the next twenty years as part of the European Integrated Carbon Observation System (ICOS, www.icos-infrastructure.eu/). This long-standing co-ordinated European network, placed across several important biomes, has already documented dramatic inter-annual variability in the amount of CO₂ sequestered over the growing season (Delpierre et al., 2009b; Le Maire et al., 2010; Osborne et al., 2010; Wu et al., 2012) and witnessed both the short-lived and long-term impacts of disturbance (Kowalski et al., 2004), heat waves (Ciais et al., 2005) and management practices (Kutsch et al., 2010; Magnani et al., 2007; Soussana et al., 2007) on the carbon and water balance of terrestrial ecosystems. As a direct result of such an observational network, it is now possible to estimate with greater confidence how evapotranspiration (ET) and net ecosystem CO₂ exchange (NEE) have responded to changes in climate over recent years (Beer et al., 2010; Jung et al., 2010) and better constrain our predictions of how ecosystems are likely to respond in the future to changes in climate using land surface and biogeochemical cycle models (Friend et al., 2007; Krinner et al., 2005).

7983

The growth of new leaves every year is clearly signalled in atmospheric CO₂ concentration records and exerts a strong control on both spatial and temporal patterns of carbon (C) sequestration and water cycling (Keeling et al., 1996; Piao et al., 2008). Hence, for the purpose of understanding patterns and processes controlling C and water budgets across a broad range of scales, there are obvious advantages in creating explicit links between flux monitoring, phenological observation and biogeochemical studies (Ahrends et al., 2009; Baldocchi et al., 2005; Kljun, 2006; Lawrence and Slingo, 2004; Richardson et al., 2007; Wingate et al., 2008). Leaf phenology has fascinated human observers for centuries and is related to external signals such as temperature or photoperiod (Aono and Kazui, 2008; Demarée and Rutishauser, 2009; Linkosalo et al., 2009). In the modern era, phenology has gained a new impetus, as people realised that such records must be sustained over many years to reveal subtle changes in plant phenology in response to climate change (Rosenzweig et al., 2007) and improve our understanding of the abiotic but also biotic (metabolic and genetic) triggers that determine seasonal changes in plant development. Currently, descriptions of phenology in dynamic vegetation models are poor and need to be improved and tested against long-term field observations if we are to predict the impact of climate change on ecosystem function and CO₂ sequestration (Keenan et al., 2014b; Kucharik et al., 2006; Richardson et al., 2011).

Variations in the concentrations of pigments and spectral properties of leaves also provide a valuable mechanistic link to changes in plant development and photosynthetic rates when interpreted with models such as PROSAIL that combine our knowledge of radiative transfer through forest canopies and leaf mesophyll cells with leaf biochemistry (Jacquemoud and Baret, 1990; Jacquemoud et al., 2009). Automated techniques to detect and assimilate changes in the optical signals of leaves either near the canopy or remotely from space in conjunction with the coupling of radiative transfer models with biogeochemical models will help to improve the representation of leaf phenology and physiology in dynamic vegetation models (Garrity et al., 2011; Hilker et al., 2011; Klosterman et al., 2014).

7984

This paper aims to synthesise data from flux sites across Europe where researchers have embraced the opportunity to establish automatic observations of phenological events by mounting digital cameras and recording daily (or even hourly) images of the vegetation throughout the seasons. We examine whether coherent seasonal changes in digital image properties can be observed at the majority of sites even if camera types and configuration are not yet harmonised and calibration procedures are not fully developed. In this work we asked the following questions (i) how well can digital images be automatically processed to reveal the key phenological events such as leaf out, flowering, leaf fall, or land management practices such as mowing and harvesting; and (ii) can we provide a mechanistic link between digital images, leaf phenology and the physiological performance of leaves in the canopy? To address the second question, we adapted the model PROSAIL (Jacquemoud and Baret, 1990; Jacquemoud et al., 2009) to simulate the seasonal changes in red, green and blue signals detected by digital cameras above canopies and performed sensitivity analysis of these signals to variations in canopy structure (leaf area, structure and angles) and biochemistry (leaf pigment and water content).

2 Material and methods

2.1 Study sites and camera set-up

The European network of digital cameras currently covers over 50 flux sites across Europe (Fig. 1 and Table 1). Table 1 demonstrates that a diverse selection of commercially available cameras are being used across the network. The cameras are installed in waterproof housing that is firmly attached to the flux tower some height above the top of the canopy. The cameras are generally orientated North, looking slightly down to the horizon to ensure that the majority of the image contains the vegetation of interest. Canopy images of the same scene are taken repeatedly each day, at a frequency that varies across the different sites from between 1 to 12 images day⁻¹ and stored as

7985

8 bit JPEG files (i.e. digital numbers ranging from 0 to 255). The archived images used in the present analysis are all taken between 11:00 and 13:00 LT. The camera setup is specific to each camera type but a common requirement to observe the seasonal colour fraction time-series is to set the colour balance to “fixed” mode (on the Star-dot cameras) or the white balance to “manual” mode (for the Nikon Coolpix cameras) (Mizunuma et al., 2013, 2014).

2.2 Image analysis

2.2.1 ROI selection and colour analysis

For each site, a squared region of interest (ROI) was selected from visual inspection of the images. The ROI had to be as large as possible and common to all images of the same growing season while including as many plants as possible but no soil or sky areas. Automated segmentation methods could also be used to select ROI with more complex geometries only on plant parts (e.g. Comar et al., 2012). However this would result in different ROI between images, that would be problematic for defining seasonal changes in image properties, and would also be somewhat impractical for large datasets as it would require an a posteriori check for the success of the method on each image.

Image ROIs were then analysed using the open-source image analysis software, Image-J (Image-J v1.36b; NIH, MS, USA). A customised macro was used to extract Red-Green-Blue (RGB) digital number (DN) values between 0 and 255 (n_{colour}) for each pixel of the ROI and a mean value for all pixel values in a given ROI of each image was calculated. Various colour indices can be obtained from digital image properties (Mizunuma et al., 2011), but here we used only the chromatic coordinates, called colour fraction hereafter (Richardson et al., 2007):

$$\text{Colour Fraction} = n_{\text{colour}} / (n_{\text{red}} + n_{\text{green}} + n_{\text{blue}}) \quad (1)$$

where colour is either red, green or blue.

7986

In the following we will thus refer to the “green fraction” as the mean green colour fraction for all pixels in the ROI, as opposed to the amount of pixels covered by vegetation in the entire image (Comar et al., 2012).

2.2.2 Data filtering procedure

5 Image quality is often adversely affected by rain, snow, low clouds, aerosols, fog and uneven patterns of illumination caused by the presence of scattered clouds. These influences often create noise in the trajectories of colour indices, and is an important source of uncertainty that can hamper the description of canopy seasonal variations and the derivation of robust phenological metrics from colour index time-series. To
10 remove problematic images that were affected by raindrops, snow or fog from the digital photograph analysis, we used a filtering algorithm based on the statistical properties of the time series, we used two steps to filter the raw data. The first filter, based on the deviation from a smoothed spline fit as described in Migliavacca et al. (2011), was used to remove outliers. Thereafter, we applied the method implemented in Sonnentag
15 et al. (2012), to reduce the variability of the colour fractions (Fig. 2).

2.2.3 Piecewise break point change analysis

We used a piecewise break point regression approach to extract automatically the main phenological events such as leaf emergence and senescence from the colour fraction time series (Fig. 2). The procedure is implemented in the R package *struc-*
20 *change* (Zeileis et al., 2002, 2003) and is used to detect breaks in a time series by identifying points where the multiple linear correlation coefficients shift from one stable regression relationship to another (Bai and Perron, 2003). The 95 % confidence intervals of the identified break points were then computed using the distribution function proposed by Bai (1997). To obtain credible breakpoints in complex green fraction time
25 series such as in highly managed sites (e.g. grazed or cut grasslands, multiple rotation crops) the possibility of identifying numerous peaks or breakpoints (up to 8 breaks)

7987

may be necessary. However, such a high number of break points would be excessive in natural ecosystems, and so we decided to set a maximum of five breakpoints per growing season, for both managed and natural ecosystems. We opted for a breakpoint approach over other commonly used methods to extract phenological transitions from
5 time series (i.e. thresholds, derivative methods) because it can be considered as more robust and less affected by noise in the time series (Henneken et al., 2013). This is particularly relevant for our application that encompasses a large dataset consisting of many different camera set-ups (camera type, target distance, image processing).

2.2.4 Determining phenophases by visual assessment

10 In order to relate the break point detection method to phenological phases we also visually examined images from broadleaf forest ecosystems for leafing out, senescence and leaf fall. Six pre-trained observers looked through the same daily images and used a common protocol to identify dates when (1) the majority of vegetation started leafing out (i.e. when 50 % of the ROI contains green leaves), (2) the canopy first started to
15 change colour to (first non-green colours such as yellow and orange) in autumn and (3) the last day when a few non-green leaves were still visible on the canopy before the day the branches became bare. These visually assessed dates were then averaged across observers and compared to the relevant breakpoints identifying the same phenological stage. The leafing out phase was associated to the first automatically detected
20 breakpoint, leaf senescence to the penultimate breakpoint and leaf fall to the last breakpoint. Based on this classification the key dates identified by the algorithm and visual inspection were consistently correlated with one another (Fig. 3). However, there was a tendency for the automatic algorithm to identify all the phenological transitions before the visually assessed dates, by about a week. Also, visual inspections
25 had larger standard deviations, especially during canopy senescence. Because of this systematic difference between the two methods, the breakpoints indicating the start of the growing season were in agreement with visually inspected dates to within 9 days only, and an even lower accuracy was found for leaf senescence and leaf fall (RMSE of

7988

tion were again detected by the piecewise regression approach, one around day 267 (bp3), coinciding with the period when minimum air temperatures began to fall below 0 °C and another around day 320 (bp4) coinciding with a short period of warmer temperatures (Fig. 5). Interestingly these breakpoints at the beginning (days 100–110, bp2) and the end (days 280–310, bp4) also coincided with the onset and cessation of GPP. The recovery of biochemical reactions and the reorganisation of the photosynthetic apparatus in green needles is known to be triggered when air temperature rises above 0 °C (Ensminger et al., 2008, 2004) and at about 3–4 °C at this particular site in Finland (Porcar-Castell, 2011; Tanja et al., 2003). Our results suggest that green fractions from digital images seem sensitive enough to detect these changes in the organisation of the photosynthetic apparatus of the coniferous evergreen needles.

3.1.2 Grassland and cropland ecosystems

Many land surface models still lack crop-related plant functional types and often substitute cropland areas with the characteristics of grasslands (Osborne et al., 2007; Sus et al., 2010). Our initial results from the EUROPhen network demonstrate the difficulty of teasing apart the seasonal and inter-annual developmental patterns as they are often complicated by co-occurring agricultural practices (e.g. cutting, ploughing, harvesting and changes in animal stocking density) (Fig. 6).

Overall we found that there was surprisingly little difference between the onset dates of growth for most of the permanent grassland sites, despite being located in very different locations across Europe. However the onset of the green fraction signal was considerably delayed at the sub-alpine grassland site in Torgnon compared with the other sites (Fig. 6). Torgnon also had the most compressed growing season of all the sites, encompassing a period of less than 100 days, some 100 days shorter than the other sites. These differences in growing season length between permanent grassland sites are caused by elevation (most grassland sites are situated at 1000 ± 50 m.a.s.l., while the Italian site Torgnon is located at ca. 2160 m.a.s.l.), that induced differences in temperature and snow cover and consequently the RGB signals.

7993

Management practices such as the cutting of meadows (e.g. Neustift and Frübüel) and changes in animal stocking rate (e.g. Laqueuille) also created abrupt shifts in the RGB signals that could be distinguished from digital images. For example at the Neustift site in Austria, the meadow was cut three times during the 2011 growing season (days 157, 213, 272) causing pronounced drops in the blue fraction and to a lesser extent reductions in the green and red signal (Fig. 7). These meadow cuts were clearly identified in the green fraction time-series by the breakpoint analysis (see bp3, bp4 and bp5 in Figs. 6 and 7). In addition, flowering events were frequently strong drivers of the colour signals at the Neustift site and led to gradual decreases in the red and green signals for several weeks prior to mowing (e.g. yellow flowers on days 134–156 (bp2), white flowers on days 176–212). In contrast the blue signal tended to increase in strength during flowering periods making the impact of the mowing events dramatic when they occurred (Fig. 7). If the piecewise regression algorithm was set to allow the detection of up to 8 breakpoints at those sites, flowering events were often identified as well as the mowing events but this made the detection of the start and end dates of the growing season even more challenging using automated algorithms. Sometimes up to 8 breakpoints could be observed in grassland ecosystems and frequently the first breakpoint was caused by the start of the snow free period, as opposed to the start of growth. Subsequent breakpoints typically indicated the phenology and management of the vegetation, particularly mowing, and suggest a visual inspection of images may still be necessary to clarify the nature and management causes behind breakpoints in some grassland sites.

In addition, at some sites it was not always easy to discern visually from images when a grassland started its first growth as often fresh shoots are hidden by litter and dead material from the previous year. This particular problem may lead to a slight overestimation of the start date of growth and additionally lead to a potential temporal mismatch between GPP and green-up signals. For example at the subalpine site in Torgnon the green fraction and GPP peaked at the same time of year (bp2), but the onset of the green signal in spring lagged the onset of photosynthesis by about 7–10 days (Fig. 8).

7994

Given these preliminary results at Neustift, Torgnon and the other EUROPhen sites, it appears that grassland green signals may provide some information on the variations in GPP over the season and between years as suggested by Migliavacca et al., (Migliavacca et al., 2011) and more recently Toomey et al. (2015) but an underestimation of the growing season length may also occur using our automatic breakpoint detection approach.

As mentioned above, the use of grassland characteristics to describe the phenology of different crops is common in models. However, at the same site we can see that the start of the growth period for each different crop varies widely over commonly applied rotations. For example at Lonze in Belgium we found that for individual crop types such as potato and winter wheat the patterns of the green signal were fairly similar between different years (Fig. 9). However, we could still observe variations between years such as a slightly shorter green period for the potatoes in 2014 relative to 2010 or a slightly later start to the season for winter wheat in 2013 relative to 2011.

As huge areas of Europe are dedicated to the production of crops (326 Mha) and grasslands (151 Mha) (Janssens et al., 2003) and are known to be one of the largest European sources of biospheric CO₂ to the atmosphere at a rate of about 33TgC_y⁻¹ (Schulze et al., 2009), it is increasingly important that more field observations of developmental or phenological transitions are obtained to constrain the timing and developmental rate of plants in situ and improve model simulations. Our initial results from the EUROPhen camera network show that digital repeat photography may provide a valuable assimilation dataset in the future for constraining variations in the timing of LAI changes across rotations as well as providing useful indicators of developmental transitions and agricultural practices (e.g. cutting, ploughing, harvesting and changes in animal stocking density).

3.1.3 Broadleaf forest ecosystems

Within the EUROPhen network the majority of broadleaf forest sites are deciduous and are identified easily by the RGB signals they produce. In order to present these sig-

7995

nals clearly across a range of broadleaf sites in the network it was necessary to show the seasonal patterns observed in different years across different sites mainly because there were often gaps in the images at one or more sites in each year. Despite Fig. 10 showing site data from different years, general patterns associated with broadleaf forest characteristics were observed. Typically the start of the temperate growing season coincides with a strong increase in the green signal and a decrease in the blue and red signals. Across the network the timing of this spring green-up varies slightly with latitude, usually occurring first in the southern sites and moving North with the British sites starting later than continental sites at similar latitudes (Fig. 10). The end of the growing season, identified clearly as a decrease in the green signal, varied considerably across the network. The more continental sites such as the Hainich and Lägeren deciduous forests exhibited the shortest growing season lengths, whilst the oceanic and Mediterranean sites had far longer growing seasons. A high degree of variability in the timing for colour changes in autumn is expected across temperate deciduous ecosystems (Archetti et al., 2008) despite the fact that, at least in the case of European tree species, changes in photoperiod and air temperature are usually considered the main drivers of the colouration of senescent leaves (Delpierre et al., 2009a; Keskitalo et al., 2005; Menzel et al., 2006).

Interestingly, the evergreen broadleaf forests at the Mediterranean sites displayed similar RGB seasonal variations (Fig. 10b). However, the peak in the green fraction values were observed somewhat later in spring compared to those of the deciduous broadleaf sites. These maximum green fraction values are most probably linked to the production of new leaves that typically occurs at this period in Holm Oak (García-Mozo et al., 2007; La Mantia et al., 2003). Interestingly, a strong decrease in the green fraction was observed prior to the peak at the Spanish site, Majadas del Tieter. Similar, patterns in NDVI time-series have been observed around the same period, at the Puechabon site but for different years to the one studied here (2006–2008; Soudani et al., 2012). This drop in NDVI was explained by the shedding of old leaves coinciding with the period of leaf sprouting in spring. However, on inspection of the Spanish site

7996

photos (Fig. S5) we found that the canopy during this period was covered in conspicuous male catkin-type flowers that appear yellow-brown in the images (Fig. 10). These flowering events are critical for the production of acorns, that randomly alternate between mast and low production years (Vázquez et al., 1990; Espárrago et al., 1992).
5 Thus, in the case of the Spanish site at least, the strong decrease in the green fraction seemed dominated by a male flowering event, in addition to the shedding of old leaves. In the case of the Puechabon site, visual inspection of the photos did not detect a strong flowering event, however, the camera is located slightly further away from the canopy making it difficult to detect flowers easily by eye. However, phenological records
10 maintained at the site indicate that the period between bp2 and bp3 when the green signal slightly decreases, coincides with the start and end of the male flowering period, as well as leaf fall. In contrast, the signal between bp3 and bp4 indicates the period of leaf flushing for this year. Further studies comparing NDVI signals with digital images should allow us to understand better the observed variations in both signals and their
15 link to phenological events such as flowering and litterfall in evergreen broadleaves and how these vary between years in response to climate.

For broadleaf deciduous (and to some extent evergreen) species our breakpoint approach also detected a significant decline in the green fraction a few weeks after leaf emergence and well before leaf senescence (Figs. 2 and 10). This pattern in the green
20 fraction has also been observed for a range of deciduous tree species in Asia and the USA (Hufkens et al., 2012; Ide and Oguma, 2010; Keenan et al., 2014a; Nagai et al., 2011; Saitoh et al., 2012; Sonnentag et al., 2012; Toomey et al., 2015; Yang et al., 2014). In addition, this feature has also been observed at the leaf scale using scanned images of leaves (Keenan et al., 2014a; Yang et al., 2014) and at the regional
25 scale for a number of deciduous forest sites using MODIS surface reflectance products (Hufkens et al., 2012; Keenan et al., 2014a). The causes that underlie the shape and duration of this large peak at the beginning of the growing season presently remain unclear. Recent camera studies that have also measured either leaf or plant area index at the same time have found no dramatic reductions in leaf area during this rapid

7997

decline in the green fraction following budburst (Keenan et al., 2014a; Nagai et al., 2011). At two of the deciduous sites within our network, Alice Holt and Sørø (Fig. 4), daily PAR transmittance was also measured providing a suitable proxy for changes in canopy leaf area. In both cases no decrease in the LAI proxy was detected during the
5 decrease of the green signal shortly after budburst. If this decrease in the green signal after leaf growth is not caused by a reduction in the amount of foliage in most cases, it is likely associated with either changes in the concentration and phasing of the different leaf pigments or changes in the leaf angle distribution. These different hypotheses are tested in the next section.

10 3.2 Modelling ecosystem RGB signals

3.2.1 Sensitivity analysis of model parameters

Using the PROSAIL model as described above, with the camera sensor specifications of the Alice Holt oak site (see Fig. S1) we performed three different sensitivity analyses of the simulated RGB fractions to the 13 model parameters (Table 2). All sensitivity
15 analyses consisted of a Monte Carlo simulation of between 2000 and 10 000 runs each. For the first analysis the model was allowed to freely explore different combinations of the parameter space over the range of values commonly found in the literature and with no constraints on how the parameters were related to each other (all parameters being randomly and uniformly distributed). The results from this initial sensitivity analysis
20 indicated that the RGB signals were sensitive to four parameters: the leaf chlorophyll ([Chl]), carotenoid ([Car]) and brown contents (C_{brown}) and the leaf structural parameter (N) (see Supplement, Fig. S6). In contrast the simulated RGB signals were relatively insensitive to leaf mass (LMA), leaf water content (EWT) and, to some extent, to LAI (above a value of ca. 1). This sensitivity analysis also nicely demonstrates how measurements of NDVI made above canopies are most strongly influenced by LAI and to
25 a slightly lesser extent by leaf pigment contents. The model also demonstrated that the

7998

impact of diffuse light or leaf inclination angle was negligible for the green signal but not for the blue and red fractions (Fig. S6).

In a second sensitivity analysis we refined our assumptions on how certain parameters were likely to vary with one another in spring during the green-up. For this, we fixed all parameters to values typical for English oak during spring conditions (Demarez et al., 1999; Kull et al., 1999), except for LAI and the concentrations of chlorophyll and carotenoid. We then imposed two further conditions stating that (1) leaf chlorophyll contents increased in proportion to LAI (i.e. the ratio of [Chl]/LAI was normally distributed) and (2) carotenoid and chlorophyll contents also increased proportionally (i.e. [Car]/[Chl] was normally distributed around $30 \pm 15\%$). This ratio between pigment contents is commonly found in temperate tree species. This second sensitivity analysis revealed clearly how the RGB fractions would likely respond to LAI, chlorophyll and carotenoid contents during the spring green-up (Fig. 11). Firstly, we observed that the RGB signals were insensitive to the full range of LAI variations typically found in deciduous forests. Most of the sensitivity in the green signal was found at very low values of LAI (< 2), whereafter the signal became insensitive. Whereas the NDVI signal was sensitive throughout the full range of typical LAI values. For the range of likely [Chl] taken from the literature for oak species (Demarez et al., 1999; Gond et al., 1999; Percival et al., 2008; Sanger, 1971; Yang et al., 2014), our simulations indicated that the sharp increase in the green signals observed by the camera sensors during leaf out are mostly caused by an increase in [Chl]. More interestingly, and contrary to our previous analysis where changes in [Chl] and [Car] were not correlated (Fig. S6), this new analysis clearly shows that, when [Chl] reached ca. $30 \mu\text{g cm}^{-2}$, the green signal begins to respond negatively to a further increase in [Chl]. This is because in this simulation an increase in [Chl] is accompanied by an increase in carotenoids and the green fraction responds negatively to an increase in [Car] (Fig. 11). Another interesting feature of this sensitivity analysis is how the dependence of NDVI on pigment content was greater when we imposed the two constraints described above. This preliminary investigation with the PROSAIL model therefore suggests that the sharp reduction in

7999

the green fraction commonly observed after budburst in deciduous forests is mostly driven by an increase in leaf pigment concentrations.

3.2.2 Modelling seasonal RGB patterns mechanistically

Using the adapted PROSAIL model and a few assumptions on how model parameters varied over the season (Table 2, Fig. 12) we investigated the ability of the PROSAIL model to simulate seasonal variations of the RGB signals measured by two different cameras installed at the Alice Holt site. For this a proxy for seasonal variations in LAI was obtained by fitting a relationship to values of LAI estimated from measurements of transmittance as described in Mizunuma et al. (2013), while the expected range and seasonal variations of [Chl], [Car], C_{brown} and N were estimated from several published studies on oak leaves (Demarez et al., 1999; Gond et al., 1999; Percival et al., 2008; Sanger, 1971; Yang et al., 2014), as summarised in Table 2. We also manually adjusted the parameter B_{RGB} in Eq. (4) to match the RGB values measured by the camera during the winter period prior to budburst (highlighted by the thick grey bar in Fig. 12).

Using this simple model parameterisation, the model was able to capture relatively well the seasonal pattern and absolute magnitude of the three colour signals, including the spring “green hump” (Fig. 12). As anticipated from our sensitivity analysis (Fig. 11) we found that at the beginning of the growing season the initial rise in the green signal is dominated by small changes in LAI and [Chl], whilst the small decrease in the green signal that follows is most likely caused by the further increase of [Chl] and [Car]. This period is also characterised by a strong decrease in the red signal and a strong increase in the blue fraction that distinguishes it clearly from the effect of changes in LAI (as blue and green signals remain constant at LAI > 2). Interestingly the maximum green signal observed by the camera coincides with the time when LAI reached half of its maximum value (dotted line on graphs), rather than when [Chl] is maximum. This theoretical result is consistent with pigment concentration data from other recent studies (Keenan et al., 2014a; Yang et al., 2014). Our analysis also indicates that the time when maximum [Chl] and/or [Car] is attained coincides more with the end of the green

8000

ever, for this step to proceed further, the network should address several technical considerations.

5 Firstly, the digital cameras in our European network are currently uncalibrated instruments unlike other commonly used radiometric instruments. In addition, these cameras are deployed in the field and are often exposed to harsh environmental conditions. Thus their characteristics may drift over time. For example although the CMOS sensors (commonly found in the cameras of our network) do not age quickly over periods of several years, the colour separation filters on the sensor plate may age after time from UV exposure. Most commercial cameras already contain UV filter protection and in addition they are protectively housed from the elements and sit behind a glass shield that protects the camera from the damage by UV or other environmental conditions, such as water. Also, the studies of Sonnentag et al. (2012) and Mizunuma et al. (2013, 2014) demonstrated that different camera brands and even different cameras of the same brand that produce different colour fraction time-series reflecting differences in their spectral response still produce coherent phenological metrics. Nonetheless, it would be useful to develop a calibration scheme by digital photography of radiometrically characterised colour sheets such as those used to detect the health and nutritional status of plants (Mizunuma et al., 2014) whilst the camera is in the field and exposed to a variety of light conditions. However, the deployment of such a colour checker for long-term continuous monitoring is problematic as the spectral quality of the colour checker will alter over time as particles, such as dust and insects, accumulate on its surface. An alternative solution could involve routinely checking for sensor drift using images taken during the winter months of different years. For example, at least in the case of deciduous broadleaf species, one or two months before the beginning of the growing season (see thick grey bar in Fig. 12, fourth panel), the RGB signals tend to display relatively constant values. Provided the camera does not move and the colour balance settings are not changed, this period could be used to detect problems with the camera when compared over several years. At Alice Holt where two cameras have been operating for at least 5 years we have found no evidence for such drift using winter time

8003

values (data not shown). Ideally, it would be desirable to use only digital cameras from manufacturers that provide information on the spectral characteristics of the sensors, filters and algorithms used, or to measure routinely the spectral response of individual cameras within the network as the cameras age.

5 Secondly, digital camera studies have typically focussed on using the green fraction to deduce the dates of canopy green-up and senescence. The green fraction has been preferred because its signal-to-noise ratio is higher in vegetated ecosystems. For this very reason, and because of inter-pixel dependencies caused by the cameras built-in image processing, we recommend setting the camera up so that the images do not contain too much sky, ideally less than 20%. In addition, as demonstrated in this study, combining the information of all three colour signals may provide more useful information on canopy physiology, phenology and management impacts. However, to look at these particular signals we must understand the effects of other environmental factors that can impact the day-to-day variability of the RGB colour fractions. In particular, colour signals are sensitive to the spectral properties of the incoming light and thus to the percentage of diffuse radiation. Using the PROSAIL model we explored the impact of diffuse radiation on the RGB signals at the Alice Holt site and found that the red and blue fractions were much more affected by rapid changes in sky conditions than the green fraction. Also by incorporating the day-to-day variations in diffuse radiation at the site the model did not reproduce better the red and blue fractions, even for cloud-free conditions (Fig. 14), demonstrating that the influence of diffuse light was not easy to account for in the model. This can be problematic as the percentage of diffuse light, unlike other variables such as leaf area index or pigment concentrations, can change dramatically from one day to the next. For this reason, the green fraction is probably the best suited signal for detecting rapid changes in leaf area and pigment concentrations, at least within their lower range of values (0–2 for LAI and 0–30 $\mu\text{g cm}^{-2}$ for [Chl]). However, these are only preliminary results that will need to be thoroughly checked for the different cameras across the entire network.

8004

Lastly, cameras within the network are so far not thermally regulated. Our preliminary results using the two most commonly used cameras in the networks (Stardot and Nikon Coolpix) seem to indicate that images are not sensitive to contrasting temperatures. This point will certainly need to be addressed more thoroughly in future studies and could be addressed by taking black images periodically to assess the level of instrument noise and its relationship with temperature. If this could be achieved then it would be possible to at least reduce noise in the signals caused by temperature.

4 Conclusions

This synthesis analysis of the European camera network demonstrates that using digital repeat photography at a daily resolution can aid the automatic identification of inter-annual variations in climate-driven vegetation status such as the emergence of new foliage (i.e. bud burst, regrowth), flowering, fruit development, leaf senescence and leaf abscission. Furthermore, agricultural practices are captured well by the camera providing a useful archive of images and colour signal changes that can be interrogated with complementary flux datasets. In the long term such datasets collected across the different networks of flux sites will become invaluable for investigating in detail the connections between climate and growing season length, and will contribute to a better understanding of the underlying controls on plant development and how these vary between plant functional types, species and location.

In addition, we suggest that, by combining all three RGB colour fractions and mechanistic radiative transfer models, these digital archives might also be used to quantify changes in the plants' physiological status. This technological breakthrough will provide a means of increasing our understanding of how canopy pigment contents vary between ecosystems and with climate and improve predictions of the CO₂ sequestration period and potential of terrestrial ecosystems.

8005

**The Supplement related to this article is available online at
doi:10.5194/bgd-12-7979-2015-supplement.**

Acknowledgements. Lisa Wingate was supported through a CarboEurope-IP grant awarded to John Grace (University of Edinburgh), a Marie Curie Intra-European Fellowship (LATIS) awarded to L. Wingate and a NERC Advanced Research Fellowship awarded to L. Wingate. Salary for Toshie Mizinuma and the equipping of several sites within the European network with cameras was kindly supported through a Jim Gray Seed Trust Award from Microsoft Research awarded to L. Wingate. Edoardo Cremonese acknowledges financial support from the PhenoALP project, an Interreg project co-funded by the European Regional Development Fund, under the operational program for territorial cooperation Italy-France (ALCOTRA) 2007–2013. The Alice Holt site is funded by the UK Forestry Commission, and the StarDot camera installation was funded through the Life + FutMon project (LIFE07 ENV/D/000218) of the European Commission. Manuela Balzarola acknowledges financial support from the EU-project Geoland2. Andreas Ibrom received funding by the Danish strategic research project ECOCLIM and the EU project CARBO-extreme, whilst installation of the webcam was initiated and funded by the EU infrastructure project IMECC. We also kindly acknowledge fieldwork funding from the British Embassy Tokyo and the British Council UK-Japan 2008 collaborative Project Grant Award, GHG Europe and STSM support for T. Mizinuma from the EUROSPEC Cost Action ES0903. We also thank the Phenological Eyes Network and the US Phenocam Network and especially Andrew Richardson and Shin Nagai for their assistance and encouragement developing the European network. We are also grateful to Daniel Lawton for his fast response time to questions regarding the technical details for the Stardot camera. Finally, we are sincerely grateful to the ongoing support of the European Flux database team and the FLUXNET research community for their continuous co-operation, assistance and participation in the activities of the camera network.

References

Ahrends, H. A., Etzold, S., Kutsch, W., Stoeckli, R., Bruegger, R., Jeanneret, F., Wanner, H., Buchmann, N., and Eugster, W.: Tree phenology and carbon dioxide fluxes: use of digital

8006

- photography for process-based interpretation at the ecosystem scale, *Clim. Res.*, 39, 261–274, 2009.
- Aono, Y. and Kazui, K.: Phenological data series of cherry tree flowering in Kyoto, Japan, and its application to reconstruction of springtime temperatures since the 9th century, *Int. J. Climatol.*, 28, 905–914, 2008.
- 5 Archetti, M.: Phylogenetic analysis reveals a scattered distribution of autumn colours, *Ann. Bot.-London*, 103, 703–713, 2009.
- Archetti, M., Doring, T. F., Hagen, S. B., Hughes, N. M., Leather, S. R., Lee, D. W., Lev-Yadun, S., Manetas, Y., Ougham, H. J., Schaberg, P. G., and Thomas, H.: Unravelling the evolution of autumn colours: an interdisciplinary approach, *TREES*, 24, 166–173, 2008.
- 10 Aubinet, M., Moureaux, C., Bodson, B., Dufranne, D., Heinesch, B., Suleau, M., Vancutsem, F., and Vilret, A.: Carbon sequestration by a crop over a 4-year sugar beet/winter wheat/seed potato/winter wheat rotation cycle, *Agr. Forest Meteorol.*, 149, 407–418, doi:10.1016/j.agrformet.2008.09.003, 2009.
- 15 Aubinet, M., Vesala, T., and Papale, D. (Eds.): *Eddy Covariance: a Practical Guide to Measurement and Data Analysis*, Springer Atmospheric Sciences, the Netherlands, 2012.
- Bai, J.: Estimation of a change point in multiple regression models, *Rev. Econ. Stat.*, 79, 551–563, 1997.
- Bai, J. and Perron, P.: Computation and analysis of multiple structural change models, *J. Appl. Econom.*, 18, 1–22, 2003.
- 20 Baldocchi, D.: Measuring fluxes of trace gases and energy between ecosystems and the atmosphere – the state and future of the eddy covariance method, *Glob. Change Biol.*, 20, 3600–3609, doi:10.1111/gcb.12649, 2014.
- Baldocchi, D. D., Falge, E., Gu, L., Olson, R., Hollinger, D., Running, S., Anthoni, P., and Bernhofer, C.: FLUXNET: a new tool to study the temporal and spatial variability of ecosystem-scale carbon dioxide, water vapor, and energy flux densities, *B. Am. Meteorol. Soc.*, 82, 2415–2434, 2001.
- 25 Baldocchi, D. D., Black, T. A., Curtis, P. S., Falge, E., Fuentes, J. D., Granier, A., Gu, L., Knohl, A., Pilegaard, K., Schmid, H. P., Valentini, R., Wilson, K., Wofsy, S., Xu, L., and Yamamoto, S.: Predicting the onset of net carbon uptake by deciduous forests with soil temperature and climate data: a synthesis of FLUXNET data, *Int. J. Biometeorol.*, 49, 377–387, 2005.

8007

- Beer, C., Reichstein, M., Tomelleri, E., Ciais, P., Jung, M., Carvalhais, N., Rödenbeck, C., Altaf Arain, M., Baldocchi, D., Bonan, G. B., Bondeau, A., Cescatti, A., Lasslop, G., Lindroth, A., Lomas, M., Luysaert, S., Margolis, H., Oleson, K. W., Rouspard, O., Veenendaal, E., Viovy, N., Williams, C., Woodward, F. I., and Papale, D.: Terrestrial gross carbon dioxide uptake: global distribution and covariation with climate, *Science*, 329, 834–838, 2010.
- 5 Ciais, P., Reichstein, M., Viovy, N., Granier, A., Ogee, J., Allard, V., Aubinet, M., Buchmann, N., Bernhofer, C., Carrara, A., Chevalier, F., de Noblet, N., Friend, A., Friedlingstein, P., Grünwald, T., Heinesch, B., Keronen, P., Knohl, A., Krinner, G., Loustau, D., Manca, G., Matteucci, G., Miglietta, F., Ourcival, J.-M., Papale, D., Pilegaard, K., Rambal, S., Seufert, G., Soussana, J.-F., Sanz, M. J., Schulze, E.-D., Vesala, T., and Valentini, R.: Europe-wide reduction in primary productivity caused by the heat and drought in 2003, *Nature*, 437, 529–533, 2005.
- 10 Comar, A., Burger, P., de Solan, B., Baret, F., Daumard, F., and Hanocq, J.-F.: A semi-automatic system for high throughput phenotyping wheat cultivars in-field conditions: description and first results, *Funct. Plant Biol.*, 39, 914–924, 2012.
- Delpierre, N., Dufrene, E., Soudani, K., Ulrich, E., Cecchini, S., Boe, J., and Francois, C.: Modelling interannual and spatial variability of leaf senescence for three deciduous tree species in France, *Agr. Forest Meteorol.*, 149, 938–948, 2009a.
- 15 Delpierre, N., Soudani, K., François, C., Köstner, B., Pontailier, J.-Y., Nikinmaa, E., Misson, L., Aubinet, M., Bernhofer, C., Granier, A., Grünwald, T., Heinesch, B., Longdoz, B., Ourcival, J.-M., Rambal, S., Vesala, T., and Dufrêne, E.: Exceptional carbon uptake in European forests during the warm spring of 2007: a data-model analysis, *Glob. Change Biol.*, 15, 1455–1474, 2009b.
- 20 Demarée, G. R. and Rutishauser, T.: Origins of the Word “Phenology”, *EOS TRANS. AGU*, 90, 291, doi:10.1029/2009EO340004, 2009.
- Demarez, V., Gastellu-Etchegorry, J. P., Mougou, E., Marty, G., Proisy, C., Dufrêne, E., and Le Dantec, V.: Seasonal variation of leaf chlorophyll content of a temperate forest. Inversion of the PROSPECT model, *Int. J. Remote Sens.*, 20, 879–894, 1999.
- 25 Ensminger, I., Sveshnikov, D., Campbell, D. A., Funk, C., Jansson, S., Lloyd, J., Shibistova, O., and Oquist, G.: Intermittant low temperatures constrain spring recovery of photosynthesis in boreal Scots pine forests, *Glob. Change Biol.*, 10, 995–1008, 2004.

8008

- Ensminger, I., Schmidt, L., and Lloyd, J.: Soil temperature and intermittent frost modulate the rate of recovery of photosynthesis in Scots pine under simulated spring conditions, *New Phytol.*, 177, 428–442, 2008.
- Farrell, J., Catrysse, P. B., and Wandell, B.: Digital camera simulation, *Appl. Optics*, 51, A80–A90, 2012.
- 5 Francois, C., Ottlé, C., Olioso, A., Prévot, L., Bruguier, N., and Ducros, Y.: Conversion of 400–1100 nm vegetation albedo measurements into total shortwave broadband albedo using a canopy radiative transfer model, *Agronomie*, 22, 611–618, doi:10.1051/agro:2002033, 2002.
- 10 Friend, A. D., Arneth, A., Kiang, N. Y., Lomas, M., Ogee, J., Rodenbeck, C., Running, S. W., Santaren, J.-D., Sitch, S., Viovy, N., Ian Woodward, F., and Zaehle, S.: FLUXNET and modelling the global carbon cycle, *Glob. Change Biol.*, 13, 610–633, doi:10.1111/j.1365-2486.2006.01223.x, 2007.
- Galvagno, M., Wohlfahrt, G., Cremonese, E., Rossini, M., Colombo, R., Filippa, G., and Migliavacca, M.: Phenology and carbon dioxide source/sink strength of a subalpine grassland in response to an exceptionally short snow season, *Environ. Res. Lett.*, 8, 25008, doi:10.1088/1748-9326/8/2/025008, 2013.
- García-Mozo, H., Gómez-Casero, M. T., Domínguez, E., and Galán, C.: Influence of pollen emission and weather-related factors on variations in holm-oak (*Quercus ilex* subsp. *ballota*) acorn production, *Environ. Exp. Bot.*, 61, 35–40, 2007.
- 20 Garrity, S. R., Bohrer, G., Maurer, K. D., Mueller, K. L., Vogel, C. S., and Curtis, P. S.: A comparison of multiple phenology data sources for estimating seasonal transitions in deciduous forest carbon exchange, *Agr. Forest Meteorol.*, 151, 1741–1752, 2011.
- Gond, V., De Pury, D. G. G., Veroustraete, F., and Ceulemans, R.: Seasonal variations in leaf area index, leaf chlorophyll, and water content; scaling-up to estimate fAPAR and carbon balance in a multilayer, multispecies temperate forest, *Tree Physiol.*, 19, 673–679, 1999.
- Henneken, R., Dose, V., Schleip, C., and Menzel, A.: Detecting plant seasonality from webcams using Bayesian multiple change point analysis, *Agr. Forest Meteorol.*, 168, 177–185, 2013.
- Hilker, T., Gitelson, A., Coops, N. C., Hall, F. G., and Black, T. A.: Tracking plant physiological properties from multi-angular tower-based remote sensing, *Oecologia*, 165, 865–876, doi:10.1007/s00442-010-1901-0, 2011.
- 30

8009

- Hufkens, K., Friedl, M., Sonnentag, O., Braswell, B. H., Milliman, T., and Richardson, A. D.: Linking near-surface and satellite remote sensing measurements of deciduous broadleaf forest phenology, *Remote Sens. Environ.*, 117, 307–321, 2012.
- Ide, R. and Oguma, H.: Use of digital cameras for phenological observations, *Ecol. Inform.*, 5, 339–347, 2010.
- 5 Jacquemoud, S. and Baret, F.: PROSPECT: a model of leaf optical properties spectra, *Remote Sens. Environ.*, 34, 75–91, 1990.
- Jacquemoud, S., Verhoef, W., Baret, F., Bacour, C., Zarco-Tejada, P. J., Asner, G. P., Francois, C., and Ustin, S. L.: PROSPECT + SAIL models: a review of use for vegetation characterization, *Remote Sens. Environ.*, 113, 556–566, 2009.
- 10 Janssens, I. A., Lankreijer, H., Matteucci, G., Kowalski, A. S., Buchmann, N., Epron, D., Pilegaard, K., Kutsch, W., Longdoz, B., Grünwald, T., Montagnani, L., Dore, S., Rebmann, C., Moors, E. J., Grelle, A., Rannik, Ü., Morgenstern, K., Oltchev, S., Clement, R., Gudmundsson, J., Minerbi, S., Berbigier, P., Ibrom, A., Moncrieff, J., Aubinet, M., Bernhofer, C., Jensen, N.-O., Vesala, T., Granier, A., Schulze, E.-D., Lindroth, A., Dolman, A. J., Jarvis, P. G., Ceulemans, R., and Valentini, R.: Productivity overshadows temperature in determining soil and ecosystem respiration across European forests, *Glob. Change Biol.*, 7, 269–278, 2001.
- 15 Janssens, I. A., Freibauer, A., Ciais, P., Smith, P., Nabuurs, G.-J., Folberth, G., Schlamadinger, B., Hutjes, R. W. A., Ceulemans, R., Schulze, E. D., Valentini, R., and Dolman, A. J.: Europe's terrestrial biosphere absorbs 7 to 12 % of European anthropogenic CO₂ emissions, *Science*, 300, 1538–1542, 2003.
- Jung, M., Reichstein, M., Ciais, P., Seneviratne, S. I., Sheffield, J., Goulden, M. L., Bonan, G., Cescatti, A., Chen, J., de Jeu, R., Dolman, A.J., Eugster, W., Gerten, D., Gianelle, D., Gobron, N., Heinke, J., Kimball, J., Law, B.E., Montagnani, L., Mu, Q., Mueller, B., Oleson, K., Papale, D., Richardson, A. D., Rouspard, O., Running, S., Tomelleri, E., Viovy, N., Weber, U., Williams, C., Wood, E., Zaehle, S., and Zhang, K.: Recent decline in the global land evapotranspiration trend due to limited moisture supply, *Nature*, 467, 951–954, 2010.
- 25 Keeling, C. D., Chin, J. F. S., and Whorf, T. P.: Increased activity of northern vegetation inferred from atmospheric CO₂ measurements, *Nature*, 382, 146–149, 1996.
- 30 Keenan, T. F., Darby, B., Felts, E., Sonnentag, O., Friedl, M., Hufkens, K., O'Keefe, J., Klosterman, S., Munger, J. W., Toomey, M., and Richardson, A. D.: Tracking forest phenology and

8010

- seasonal physiology using digital repeat photography: a critical assessment, *Ecol. Appl.*, 24, 1478–1489, doi:10.1890/13-0652.1, 2014a.
- Keenan, T. F., Gray, J., Friedl, M. A., Toomey, M., Bohrer, G., Hollinger, D. Y., Munger, J. W., O’Keefe, J., Schmid, H. P., Wing, I. S., Yang, B., and Richardson, A. D.: Net carbon uptake has increased through warming-induced changes in temperate forest phenology, *Nature Climate Change*, 4, 598–604, doi:10.1038/NCLIMATE2253, 2014b.
- Keskitalo, J., Bergquist, G., Gardstrom, P., and Jansson, S.: A cellular timetable of autumn senescence, *Plant Physiol.*, 139, 1635–1648, 2005.
- Kljun, N., Black, T. A., Griffis, T. J., Barr, A. G., Gaumont-Guay, D., Morgenstern, K., McCaughey, J. H., and Nesic, Z.: Response of net ecosystem productivity of three boreal forest stands to drought, *Ecosystems*, 9, 1128–1144, 2006.
- Klosterman, S. T., Hufkens, K., Gray, J. M., Melaas, E., Sonnentag, O., Lavine, I., Mitchell, L., Norman, R., Friedl, M. A., and Richardson, A. D.: Evaluating remote sensing of deciduous forest phenology at multiple spatial scales using PhenoCam imagery, *Biogeosciences*, 11, 4305–4320, doi:10.5194/bg-11-4305-2014, 2014.
- Kowalski, A. S., Loustau, D., Berbigier, P., Manca, G., Tedeschi, V., Borghetti, M., Valentini, R., Kolari, P., Berninger, F., Rannik, U., Hari, P., Rayment, M., Mencuccini, M., Moncrieff, J., and Grace, J.: Paired comparisons of carbon exchange between undisturbed and regenerating stands in four managed forests in Europe, *Glob. Change Biol.*, 10, 1707–1723, doi:10.1111/j.1365-2486.2004.00846.x, 2004.
- Krinner, G., Viovy, N., Noblet-Ducoudré, N. D., Ogée, J., Polcher, J., Friedlingstein, P., Ciais, P., Sitch, S., and Prentice, I. C.: A dynamic global vegetation model for studies of the coupled atmosphere–biosphere system, *Global Biogeochem. Cy.*, 19, GB1015, doi:10.1029/2003GB002199, 2005.
- Kucharik, C. J., Barford, C. C., El Maayar, M., Wofsy, S. C., Monson, R. K., and Baldocchi, D.: A multiyear evaluation of a dynamic global vegetation model at three AmeriFlux forest sites: vegetation structure, phenology, soil temperature, and CO₂ and H₂O vapor exchange, *Ecol. Model.*, 196, 1–31, 2006.
- Kutsch, W. L., Aubinet, M., Buchmann, N., Smith, P., Osborne, B., Eugster, W., Wattenbach, M., Schrumpf, M., Schulze, E. D., Tomelleri, E., Ceschia, E., Bernhofer, C., Béziat, P., Carrara, A., Tommasi, P. D., Grünwald, T., Jones, M., Magliulo, V., Marloie, O., Moureaux, C., Olioso, A., Sanz, M. J., Saunders, M., Søgaard, H., and Ziegler, W.: The net biome production of full crop rotations in Europe, *Agr. Ecosyst. Environ.*, 139, 336–345, 2010.

8011

- La Mantia, T., Cullotta, S., and Garfi, G.: Phenology and growth of *Quercus ilex* L. in different environmental conditions in Sicily (Italy), *Ecologia mediterranea*, 29, 15–25, 2003.
- Lasslop, G., Reichstein, M., Papale, D., Richardson, A. D., Arneth, A., Barr, A. G., Stoy, P., and Wohlfahrt, G.: Separation of net ecosystem exchange into assimilation and respiration using a light response curve approach: critical issues and global evaluation, *Glob. Change Biol.*, 16, 187–208, 2010.
- Lawrence, D. M. and Slingo, J. M.: An annual cycle of vegetation in a GCM. Part I: Implementation and impact on evaporation, *Clim. Dynam.*, 22, 87–105, 2004.
- Le Maire, G., Delpierre, N., Jung, M., Ciais, P., Reichstein, M., Viovy, N., Granier, A., Ibrom, A., Kolari, P., Longdoz, B., Moors, E. J., Pilegaard, K., Rambal, S., Richardson, A. D., and Vesala, T.: Detecting the critical periods that underpin interannual fluctuations in the carbon balance of European forests, *J. Geophys. Res.*, 115, G00H03, doi:10.1029/2009JG001244, 2010.
- Lev-Yadun, S. and Holopainen, J. K.: Why red-dominated autumn leaves in America and yellow-dominated autumn leaves in Northern Europe?, *New Phytol.*, 183, 497–501, 2009.
- Linkosalo, T., Hakkinen, R., Terhivuo, J., Tuomenvirta, H., and Hari, P.: The time series of flowering and leaf bud burst of boreal trees (1846–2005) support the direct temperature observations of climatic warming, *Agr. Forest Meteorol.*, 149, 453–461, 2009.
- Magnani, F., Mencuccini, M., Borghetti, M., Berbigier, P., Berninger, F., Delzon, S., Grelle, A., Hari, P., Jarvis, P. G., Kolari, P., Kowalski, A. S., Lankreijer, H., Law, B. E., Lindroth, A., Loustau, D., Manca, G., Moncrieff, J. B., Rayment, M., Tedeschi, V., Valentini, R., and Grace, J.: The human footprint in the carbon cycle of temperate and boreal forests, *Nature*, 447, 849–851, 2007.
- Menzel, A., Sparks, T. H., Estrella, N., Koch, E., Aasa, A., Ahas, R., Alm-Kubler, K., Bissolli, P., Braslavska, O. G., Briede, A., Chmielewski, F. M., Crepinsek, Z., Curnel, Y., Dahl, A., Defila, C., Donnelly, A., Filella, Y., Jatczak, K., Mage, F., Mestre, A., Nordli, O., Penuelas, J., Pirinen, P., Remisova, V., Scheffinger, H., Striz, M., Susnik, A., Van Vliet, A. J. H., Wielgolaski, F.-E., Zach, S., and Züst, A. N. A.: European phenological response to climate change matches the warming pattern, *Glob. Change Biol.*, 12, 1969–1976, doi:10.1111/j.1365-2486.2006.01193.x, 2006.
- Migliavacca, M., Galvagno, M., Cremonese, E., Rossini, M., Meroni, M., Cogliati, S., Manca, G., Diotri, F., Busetto, L., Colombo, R., Fava, F., Pari, E., Siniscalco, C., Morra di Cella, U., and Richardson, A. D.: Using digital repeat photography and eddy covariance data to model

8012

- Schulze, E. D., Luyssaert, S., Ciais, P., Freibauer, A., Janssens, I. A., Soussana, J. F., Smith, P., Grace, J., Levin, I., Thiruchittampalam, B., Heimann, M., Dolman, A. J., Valentini, R., Bousquet, P., Peylin, P., Peters, W., Rodenbeck, C., Etiope, G., Vuichard, N., Wattenbach, M., Nabuurs, G. J., Poussi, Z., Nieschulze, J., Gash, J. H., and the CarboEurope Team: Importance of methane and nitrous oxide for Europe's terrestrial greenhouse-gas balance, *Nat. Geosci.*, 2, 842–850, 2009.
- Sonnentag, O., Hufkens, K., Teshera-Sterne, C., Young, A. M., Friedl, M., Braswell, B. H., Milliman, T., O'Keefe, J., and Richardson, A. D.: Digital repeat photography for phenological research in forest ecosystems, *Agr. Forest Meteorol.*, 152, 159–177, 2012.
- Soudani, K., Hmimina, G., Delpierre, N., Pontailleur, J.-Y., Aubinet, M., Bonal, D., Caquet, B., de Grandcourt, A., Burban, B., Flechard, C., Guyon, D., Granier, A., Gross, P., Heinesh, B., Longdoz, B., Loustau, D., Moureaux, C., Ourcival, J.-M., Rambal, S., Saint André, L., and Dufrêne, E.: Ground-based Network of NDVI measurements for tracking temporal dynamics of canopy structure and vegetation phenology in different biomes, *Remote Sens. Environ.*, 123, 234–245, 2012.
- Soussana, J. F., Allard, V., Pilegaard, K., Ambus, P., Amman, C., Campbell, C., Ceschia, E., Clifton-Brown, J., Czobel, S., Domingues, R., Flechard, C., Fuhrer, J., Hensen, A., Horvath, L., Jones, M., Kasper, G., Martin, C., Nagy, Z., Neftel, A., Raschi, A., Baronti, S., Rees, R. M., Skiba, U., Stefani, P., Manca, G., Sutton, M., Tuba, Z., and Valentini, R.: Full accounting of the greenhouse gas (CO₂, N₂O, CH₄) budget of nine European grassland sites, *Agr. Ecosyst. Environ.*, 121, 121–134, 2007.
- Sus, O., Williams, M., Bernhofer, C., Beziat, P., Buchmann, N., Ceschia, E., Doherty, R., Eugster, W., Grunwald, T., Kutsch, W., Smith, P., and Wattenbach, M.: A linked carbon cycle and crop developmental model: description and evaluation against measurements of carbon fluxes and carbon stocks at several European agricultural sites, *Agr. Ecosyst. Environ.*, 139, 402–418, 2010.
- Tanja, S., Berninger, F., Vesala, T., Markkanen, T., Hari, P., Makela, A., Ilvesniemi, H., Nikinmaa, E., Huttula, T., Laurila, T., Aurela, M., Grelle, A., Lindroth, A., Arneth, A., Shibistova, O., and Lloyd, J.: Air temperature triggers the recovery of evergreen boreal forest photosynthesis in spring, *Glob. Change Biol.*, 9, 1410–1426, 2003.
- Toomey, M., Friedl, M., Frolking, S., Hufkens, K., Klosterman, S., Sonnentag, O., Baldocchi, D., Bernacchi, C., Biraud, S. C., Bohrer, G., Brzostek, E., Burns, S. P., Coursolle, C., Hollinger, D. Y., Margolis, H. A., McCaughy, H., Monson, R. K., Munger, J. W., Pallardy, S.,

8015

- Phillips, R. P., Torn, M. S., Wharton, S., Zeri, M., and Richardson, A. D.: Greenness indices from digital cameras predict the timing and seasonal dynamics of canopy-scale photosynthesis, *Ecol. Appl.*, 25, 99–115, 2015.
- Valentini, R., Matteucci, G., Dolman, A. J., Schulze, E.-D., Rebmann, C., Moors, E. J., Granier, A., Gross, P., Jensen, N. O., Pilegaard, K., Lindroth, A., Grelle, A., Bernhofer, C., Grünwald, T., Aubinet, M., Ceulemans, R., Kowalski, A. S., Vesala, T., Rannik, Ü., Berbigier, P., Loustau, D., Guömundsson, J., Thøgerisson, H., Ibrom, A., Morgenstern, K., Clement, R., Moncrieff, J., Montagnani, L., Minerbi, S., and Jarvis, P. G.: Respiration as the main determinant of carbon balance in European forests, *Nature*, 404, 861–865, 2000.
- Verhoef, W.: Light scattering by leaf layers with application to canopy reflectance modeling: the SAIL model, *Remote Sens. Environ.*, 16, 125–141, 1984.
- Vesala, T., Launiainen, S., Kolari, P., Pumpanen, J., Sevanto, S., Hari, P., Nikinmaa, E., Kaski, P., Mannila, H., Ukkonen, E., Piao, S. L., and Ciais, P.: Autumn temperature and carbon balance of a boreal Scots pine forest in Southern Finland, *Biogeosciences*, 7, 163–176, doi:10.5194/bg-7-163-2010, 2010.
- Wilkinson, M., Eaton, E. L., Broadmeadow, M. S. J., and Morison, J. I. L.: Inter-annual variation of carbon uptake by a plantation oak woodland in south-eastern England, *Biogeosciences*, 9, 5373–5389, doi:10.5194/bg-9-5373-2012, 2012.
- Wingate, L., Richardson, A. D., Weltzin, J. F., Nasahara, K. N., and Grace, J.: Keeping an eye on the carbon balance: linking canopy development and net ecosystem exchange using a webcam, *Fluxletter*, 1, 14–17, 2008.
- Wohlfahrt, G., Hammerle, A., Haslwanter, A., Bahn, M., Tappeiner, U., and Cernusca, A.: Seasonal and inter-annual variability of the net ecosystem CO₂ exchange of a temperate mountain grassland: effects of weather and management, *J. Geophys. Res.*, 113, D8, doi:10.1029/2007JD009286, 2008.
- Wu, C., Chen, J. M., Gonsamo, A., Price, D. T., Black, T. A., and Kurz, W. A.: Interannual variability of net carbon exchange is related to the lag between the end-dates of net carbon uptake and photosynthesis: evidence from long records at two contrasting forest stands, *Agr. Forest Meteorol.*, 164, 29–38, 2012.
- Yang, X., Tang, J., and Mustard, J.: Beyond leaf color: comparing camera-based phenological metrics with leaf biochemical, biophysical and spectral properties throughout the growing season of a temperate deciduous forest, *J. Geophys. Res.-Biogeophys.*, 119, 181–191, doi:10.1002/2013JG002460, 2014.

8016

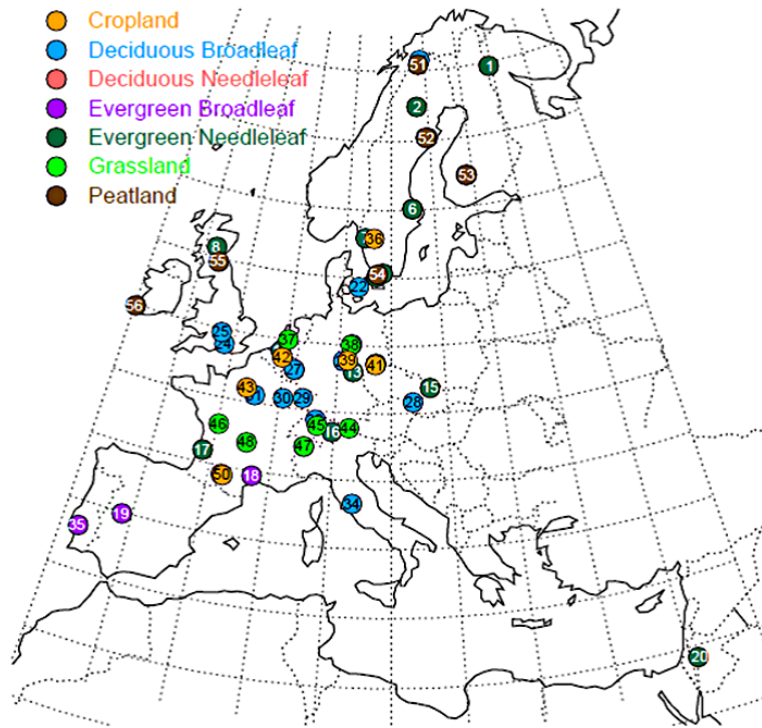


Figure 1. Distribution of operational digital cameras at flux sites across Europe for further details refer to Table 1.

8021

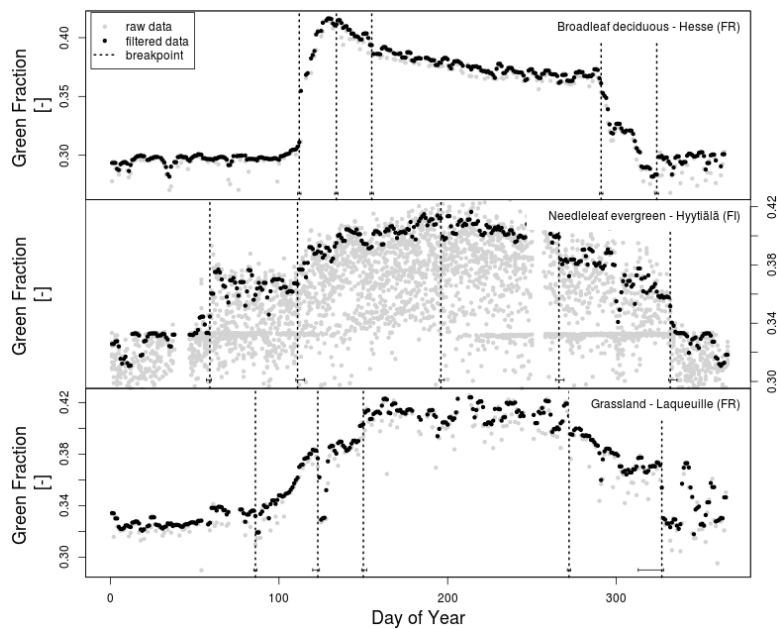


Figure 2. Green fraction time-series for the broadleaf deciduous forest, Hesse in France, the needleleaf evergreen forest Hyytiälä in Finland and the grassland Laqueuille in France, demonstrating the filtering and phenostage extraction approach used in our synthesis. Grey and black dots indicate raw and filtered data, respectively while dashed vertical lines indicate the breakpoints extracted on the green fraction time-series using the piecewise regression approach. At the bottom of each vertical line the 95% confidence interval of the breakpoint dates is also shown.

8022

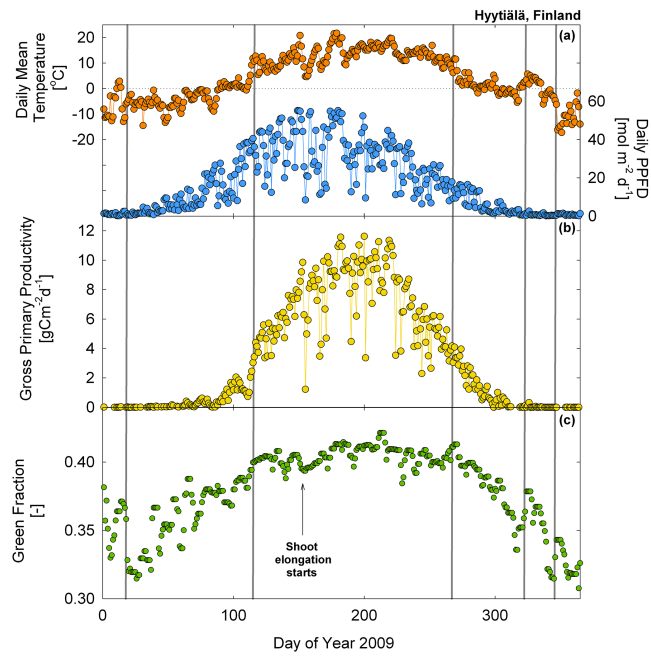


Figure 5. Time-series of (a) daily temperature, daily PPFD (b) GPP (c) green fraction variations over the year with vertical solid lines showing major breakpoint changes identifying important transitions in the green fraction over the growing season at the Hyytiälä flux site in Finland during 2009.

8025

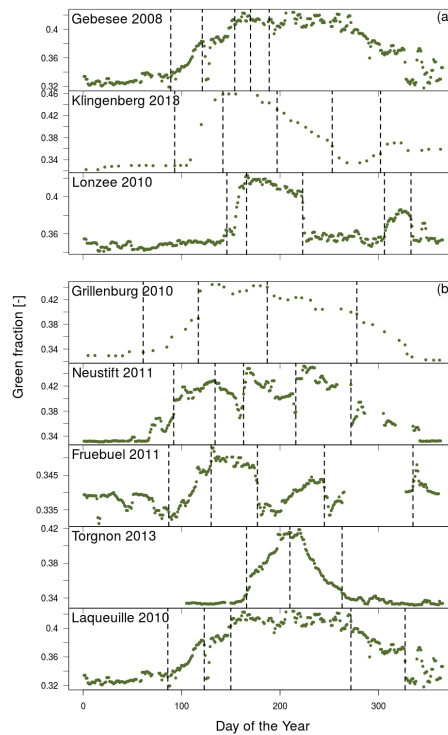


Figure 6. A latitudinal comparison of filtered green fraction time-series for a selection of (a) cropland and (b) grassland flux sites within the EUROPhen camera network with vertical dashed lines showing major breakpoint changes identifying important transitions in the green fraction over the growing season.

8026

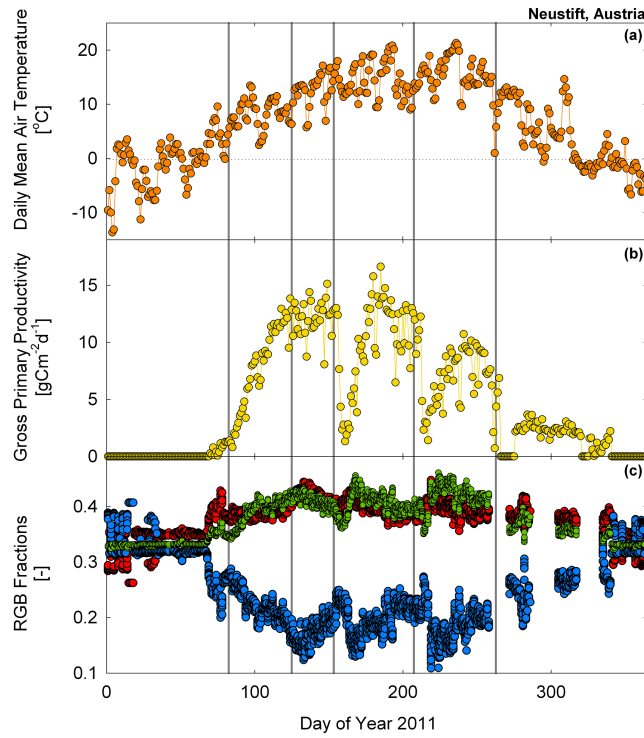


Figure 7. Impact of (a) temperature, phenology and mowing practices on (b) GPP and (c) RGB colour fractions with solid vertical lines showing major breakpoint changes identifying important transitions in the green fraction over the growing season for the alpine meadow flux site Neustift in Austria.

8027

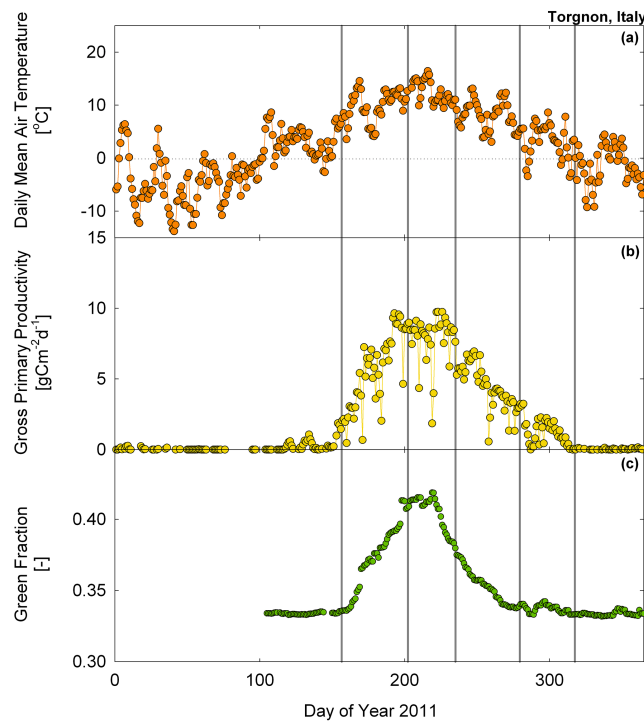


Figure 8. Time-series for the alpine grassland, Torgnon in Italy demonstrating (a) the daily mean air temperature (b) the gross primary productivity and (c) the calculated breakpoints for the green fraction using the piecewise regression approach. Vertical solid lines show major breakpoint changes identifying important transitions in the green fraction over the growing season.

8028

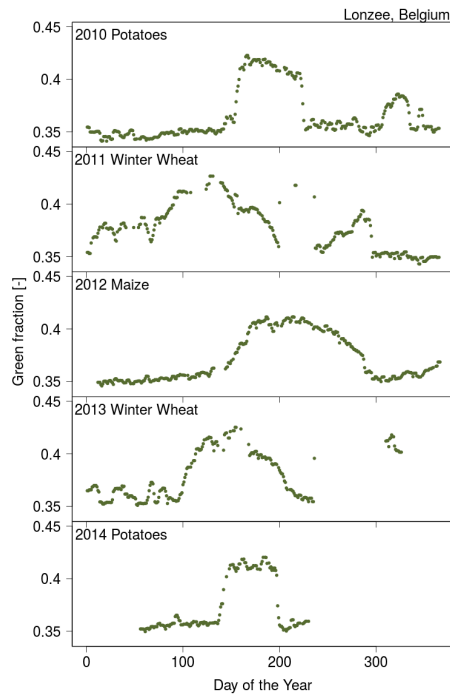


Figure 9. Impact of crop management practices and crop rotation on the green colour fractions over the growing seasons 2010–2014 for the agricultural flux site Lonzee in Germany.

8029

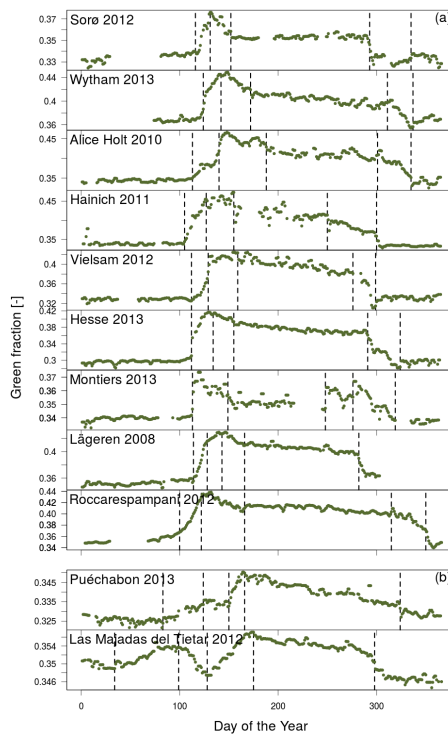


Figure 10. A latitudinal comparison of filtered green fraction time-series for a selection of (a) deciduous and (b) evergreen broadleaf forest flux sites within the European webcam network, with vertical dashed lines showing major breakpoint changes identifying important transitions in the green fraction over the growing season.

8030

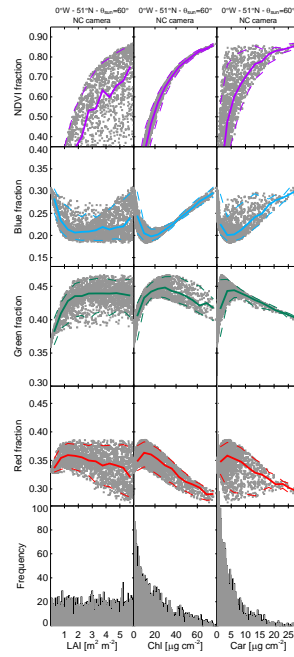


Figure 11. Sensitivity of modelled RGB fractions and NDVI for the NetCam camera at the Alice Holt deciduous broadleaf forest, as predicted by the PROSAIL model and using constrained by Chl:Car and Chl:LAI ratios (see text). All other parameters are set to standard budburst values and the solar elevation is fixed at 60°. The NDVI is computed using the camera view angle and the same wavebands as for MODIS NDVI (545–565 nm for red and 841–871 nm for near infrared).

8031

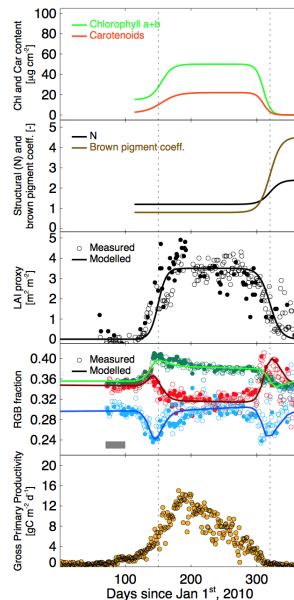


Figure 12. Time-series of modelled leaf chlorophyll (Chl), carotenoid (Car) and brown pigment (C_{brown}) contents, leaf structural parameters and modelled LAI used to predict RGB color fractions at the Alice Holt broadleaf deciduous forest for the Netcam camera and the 2010 growing season. Other parameters are as in Table 2. Proxy LAI estimates and measured RGB fractions from camera images are also shown for comparison, as well as measured daily gross primary productivity. Cloud-free conditions ($fd_{\text{diffuse}} < 0.5$) are distinguished from cloudy conditions using closed symbols. The thick grey horizontal bar indicates the period used to adjust B_{RGB} (see text).

8032

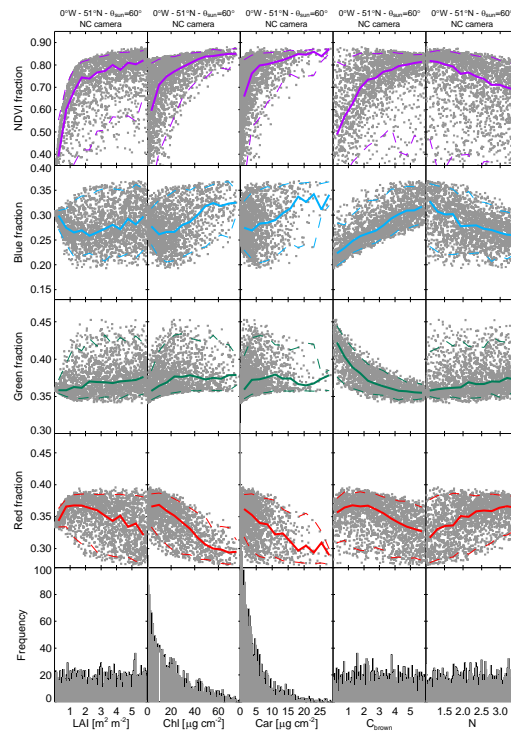


Figure 13. Results from the PROSAIL sensitivity analysis as performed in Fig. 12 except that the leaf brown pigment (C_{brown}) and structural parameter (N) are now allowed to vary independently of the other parameters, as expected during senescence.

8033

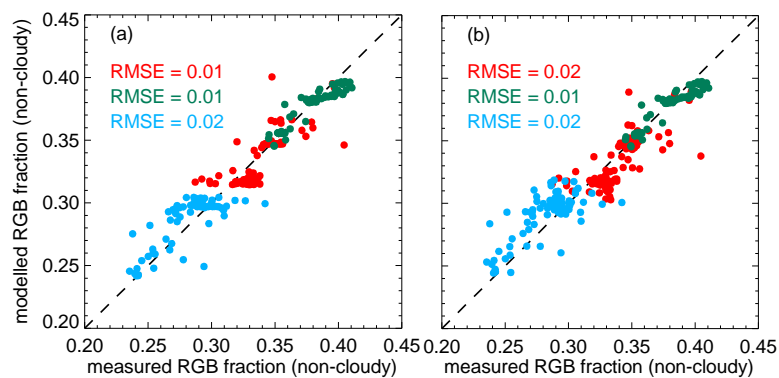


Figure 14. Modelled vs. measured RGB fractions for Alice Holt deciduous forest site during cloud-free conditions ($\varphi_{\text{diffuse}} < 0.5$) assuming (a) constant or (b) variable diffuse light conditions. The modelled values are obtained from the PROSAIL radiative transfer model as described in the text and shown in Fig. 13. The measured RGB fractions are computed from images taken by the Netcam camera system. Similar results were found for the Nikon Coolpix camera.

8034